thus does not provide a test of the hypothesis of extralunar origin. A selective study of the more deeply seated gases produced in solar flares might, however, provide such a test. By leaching away the surfaces of specific silicate grains, one might be able to study the solar flare gas content of the interior portions. However, because of possible diffusion effects, a rare gas study would be more difficult to interpret than our track evidence.

Spallogenic nuclides are produced by cosmic-ray bombardment down to a depth of ~ 1 m. From analysis of stable spallogenic rare gases, various groups have inferred an exposure age of ~ 5×10^8 years for the soil (*13–15*). This is not its absolute age but refers to the time spent within ~ 1 m of the surface. Provided deep stirring has occurred, this age can be compatible either with an early origin of the soil or with continuing production.

An extralunar origin of the grains with high track densities is consistent with Gold's dust model (*16*) of the origin of the lunar surface. We believe that the attractive features of his model outweigh the difficulties. An important and testable consequence of the model is that the grains with high track densities should also occur at much greater depths than 60 cm, perhaps orders of magnitude deeper. The desirability of a 4-m core sample such as had been planned on Apollo 13 is obvious.

The most popular model of the origin of the soil is that a regolith accumulates on a solid bedrock by comminution of chips of the bedrock resulting from meteorite impacts (*17*). Our explanation for the high track densities could be compatible with this impact model only if the extralunar infall had continued over several billion years, so as to maintain a large fraction of infallen grains with very high track densities. We believe that the simplest explanation of our results is that much of the soil developed from infall of extralunar particles (*18*).

Note added in proof: We have now directly measured the energy spectrum of Fe nuclei over a 2.5-year period by analyzing tracks recorded in a glass filter in the Surveyor 3 camera that was brought back from the moon by the Apollo 12 astronauts. We have found that the Fe/H ratio in low-energy solar particles is much higher than we had assumed from the photospheric ratio. The high Fe flux reduces but does not entirely eliminate the difficulty of accounting for the grains with high track density. An extralunar origin of part of the soil is still consistent with our observations.

D. J. BARBER*
I. HUTCHEON
P. B. PRICE

Department of Physics, University of California, Berkeley 94720

References and Notes

1. M. Maurette, P. Pellas, R. M. Walker, *Nature* **204**, 821 (1964).
2. Etched nuclear tracks of natural origin were first seen by P. B. Price and R. M. Walker [*Nature* **196**, 732 (1962)], who observed spontaneous fission tracks in terrestrial micas by electron microscopy. Etched tracks of heavy cosmic rays in extraterrestrial bodies (meteorites) were first observed by optical microscopy and reported by Maurette *et al.* [see (*1*)].
3. Further details of the x-ray analysis will be reported elsewhere.
4. G. Crozaz, U. Haack, M. Hair, M. Maurette, R. Walker, D. Woolum, in *Proceedings of the Apollo 11 Lunar Science Conference* (Pergamon, New York, 1970), vol. 3, p. 2051.
5. R. L. Fleischer, E. L. Haines, H. R. Hart, R. T. Woods, G. M. Comstock, *ibid.*, p. 2103.
6. D. Lal, D. Macdougall, L. Wilkening, G. Arrhenius, *ibid.*, p. 2295.
7. P. B. Price and D. O'Sullivan, *ibid.*, p. 2351.
8. D. J. Barber and P. B. Price, in preparation.
9. J. R. Arnold, private communication.
10. J. Hsieh and J. A. Simpson, private communication.
11. R. R. Keays, R. Ganapathy, J. C. Laul, E. Anders, G. F. Herzog, P. M. Jeffery, *Science* **167**, 490 (1970).
12. D. Heymann, A. Yaniv, J. A. S. Adams, G. E. Fryer, *ibid.*, p. 555.
13. P. Eberhart *et al.*, *ibid.*, p. 558.
14. T. Kirsten, F. Steinbrunn, J. Zähringer, *ibid.*, p. 571.
15. K. Marti, G. W. Lugmair, H. C. Urey, *ibid.*, p. 548; R. O. Pepin, L. E. Nyquist, D. Phinney, D. C. Black, *ibid.*, p. 550; C. M. Hohenberg, P. K. Davis, W. A. Kaiser, R. S. Lewis, J. H. Reynolds, in *Proceedings of the Apollo 11 Lunar Science Conference* (Pergamon, New York, 1970), vol. 2, p. 1283.
16. T. Gold, "The Nature of the Surface of the Moon" (preprint 380, Cornell University Center for Radiophysics and Space Research, Ithaca, N.Y., 1970); ———, *Proc. Amer. Phil. Soc.*, in press; ——— and S. Soter, *Science* **169**, 1071 (1970).
17. E. M. Shoemaker *et al.*, in *Proceedings of the Apollo 11 Lunar Science Conference* (Pergamon, New York, 1970), vol. 3, p. 2399.
18. After the manuscript of this report was completed, we learned of high voltage electron microscope observations of lunar crystals with track densities up to 10^{11} per square centimeter [J. Borg, J. C. Dran, L. Durrieu, C. Jouret. and M. Maurette, *Earth Planet. Sci. Lett.* **8**, 379 (1970)]. They used an acid solution that was approximately 70 times as strong as the one we used, but they reported that the tracks in their grains were not etched. It is possible that all silicates were completely dissolved in their solution, leaving only mineral grains that would require a different chemical etchant. One of their photographs was of a cristobalite grain, which we believe would not be etched in their solution.
19. We are greatly indebted to F. Borden for experimental assistance. Supported by NASA contract NAS 9-10488 and by AEC contract AT(04-3)-34.

* On leave from Department of Physics, Essex University, Colchester, U.K.

8 October 1970

Ordering of V^{2+}, Mn^{2+}, and Fe^{3+} Ions in Zoisite, $Ca_2Al_3Si_3O_{12}(OH)$

Abstract. *The presence of very small amounts of* Mn^{2+}, V^{2+}, *and* Fe^{3+} *ions in zoisite can be easily detected by the electron paramagnetic resonance technique at room temperature. The* Mn^{2+} *and* Fe^{3+} *ions are completely ordered and are probably located in the Ca(1)- and Al(II)-sites, respectively, whereas the* V^{2+} *ions probably occupy both Ca(1)- and Ca(2)-sites, with a preference for the Ca(1)-site.*

The electron paramagnetic resonance (EPR) technique, primarily used thus far in the field of solid-state physics, has been applied only recently to mineralogical problems. The EPR technique can be used to detect very small amounts of transition metal impurities [in the parts-per-million (ppm) range] in their various valence states in a diamagnetic mineral host. From the variation of the EPR spectra as a function of the crystal orientation within the

Table 1. Spin Hamiltonian parameters in zoisite.

Ion	g	$\|D\|$ (cm^{-1})	$\|E\|$ (cm^{-1})	Average $\|A\|$ (cm^{-1})	Site symmetry	Mirror plane	Angle* between principal and crystallographic axes
Mn^{2+}	2.003 ± 0.005, isotropic	$(103 \pm 5) \times 10^{-4}$	$(34 \pm 2) \times 10^{-4}$	$(85 \pm 2) \times 10^{-4}$, isotropic	*m*	(010)	5° ± 1°
V_1^{2+}	1.940 ± 0.007, isotropic	< 0.014	< 0.005	$(88 \pm 4) \times 10^{-4}$, anisotropic	*m*	(010)	7° ± 2°
V_2^{2+}	1.940 ± 0.007, isotropic	< 0.014	< 0.005	$(100 \pm 6) \times 10^{-4}$, anisotropic	1	None	
Fe^{3+}	$g_z = 1.96 \pm 0.01$	0.14 ± 0.03	$<< \|D\|$	None	*m*	(010)	44° ± 1°

* The two coordinate systems are related to each other by a rotation about the *b*-axis.

magnetic field, the local site symmetry of these ions may be determined. If the crystal structure is known, a knowledge of the local symmetry of these ions can be used to assign them to various crystallographic sites. Hence the EPR technique is a powerful tool for the study of the distribution of trace amounts of transition metal ions within various structural sites in a diamagnetic mineral. Furthermore, from the spin Hamiltonian parameters we may learn about the nature of the crystalline electric field (or ligand field) acting on these ions. The hyperfine interaction of the electrons with the nucleus or the superhyperfine interaction of the electrons with surrounding ligands gives us a measure of the covalent participation in the bonding of the transition ions with their surrounding ligands. The general theory and application have been reviewed by Abragam and Bleaney (*1*) and the applications in mineralogy have been reviewed by Ghose (*2*).

Recently, Ghose and Schindler (*3, 4*) and Wildeman (*5*) have described the distribution of Mn^{2+} between the Ca- and Mg-sites in diopsides, $CaMgSi_2O_6$, and dolomites, $CaMg(CO_3)_2$. Three types of Mn^{2+} distributions have been found in natural diopsides: (i) most Mn^{2+} in the Ca-site; (ii) most Mn^{2+} in the Mg-site; and (iii) all Mn^{2+} in the Mg-site. Natural and synthetic diopsides known to have crystallized above 900°C and containing 10 ppm of Mn^{2+} or less invariably showed all Mn^{2+} in the Mg-site. After a Californian diopside with 50 ppm Mn^{2+} initially located mostly on the Ca-site had been heated above 900°C, there was a migration of Mn^{2+} ions from the Ca-site to the Mg-site (*3*). In natural dolomites, on the other hand, only two types of Mn^{2+} distributions have been found: (i) most Mn^{2+} in the Mg-site; and (ii) almost all Mn^{2+} in the Mg-site. Heating at 700°C, under 1 kb CO_2 pressure, did not induce any Mn^{2+} migration (*4, 5*).

We report here the ordering of Mn^{2+}, V^{2+}, and Fe^{3+} ions in zoisite, $Ca_2Al_3Si_3O_{12}(OH)$, a common rock-forming silicate. The zoisite structure is orthorhombic, space group *Pnma*, with $a_0 = 16.212$ Å, $b_0 = 5.559$ Å, and $c_0 = 10.036$ Å. The structure consists of octahedral chains made up of Al(I)–O and Al(II)–O octahedra, sharing edges, running parallel to the *b*-axis; these chains are held together by isolated SiO_4 and Si_2O_7 groups and two types of CaO_7 polyhedra (*6, 7*). The structure of zoisite is shown in Fig. 1.

An EPR spectrometer (Varian E-9) has been used to record the paramagnetic resonance spectra in zoisite at room temperature near 9.3 Ghz with the magnetic field, **H**, at various angles in the (100), (010), and (001) planes. For **H** parallel to the *a*-axis, four different sets of resonance lines have been observed in a blue, gem-quality zoisite crystal from Tanzania. In Fig. 2 the single intense line at the left is due to Fe^{3+}. The intense six-line central $(-1/2 \rightarrow 1/2)$ transitions with the weak inner satellite pair $(\pm 1/2 \rightarrow \pm 3/2)$ marked *m′* and *m″* (Fig. 2, A and B) are from Mn^{2+}; the two nonequivalent eight-line central transitions marked V_1 and V_2 are from V^{2+}. The V_1 lines are more intense than the V_2 lines, an indication that the V^{2+} ions of type 1 are more abundant than the V^{2+} ions of type 2. Strong Fe^{3+} and weak Mn^{2+} lines have also been observed in zoisites from Ducktown, Tennessee; Goschen, Massachusetts; Buck County, North Carolina; and Baja California, Mexico. Pink zoisite (thulite) from Fanny Gouge Mine, Yancey County, North Carolina, also showed the presence of a considerable amount (~ 0.1 percent) of Mn^{2+}. No V^{2+} lines have been detected in any other zoisite sample.

The paramagnetic resonance spectra may be described by the spin Hamiltonian, $\mathcal{H}$, in the principal coordinate system *x, y, z*:

$$\mathcal{H} = \beta\,(g_z H_z S_z + g_x H_x S_x + g_y H_y S_y) + D\,[S_z^2 - \tfrac{1}{3}S(S+1)] + E(S_x^2 + S_y^2) + A_z S_z I_z + A_x S_x I_x + A_y S_y I_y$$

where β is the Bohr magneton, *g* is the spectroscopic splitting factor, *S* and *I* are the electronic and nuclear spins, respectively, **H** is the magnetic field, *A* is the hyperfine interaction constant, and *D* and *E* are the crystal field parameters (*1*). The spin Hamiltonian parameters and the orientation of the principal axes *x, y, z* with reference to the crystallographic axes *a, b, c* measured in the gem-quality zoisite crystal from Tanzania are listed in Table 1.

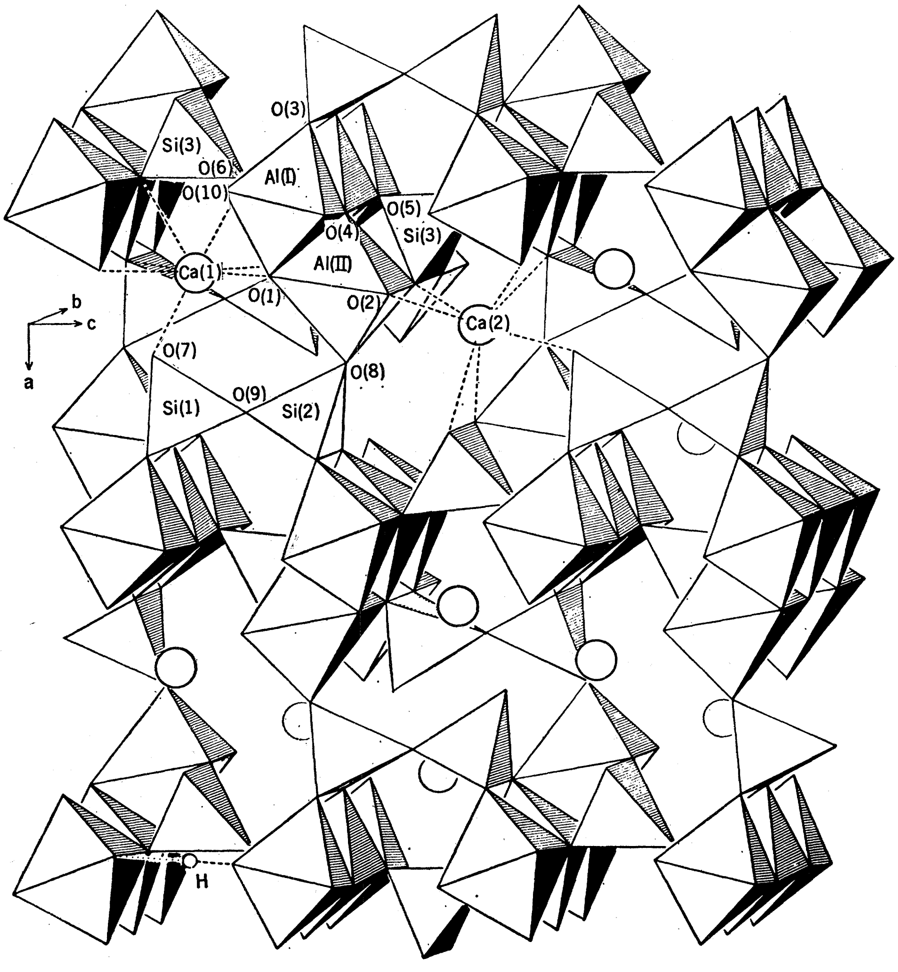

Fig. 1. Schematic diagram of the zoisite structure along the *b*-axis [modeled after the diagram of Dollase (*7*)].

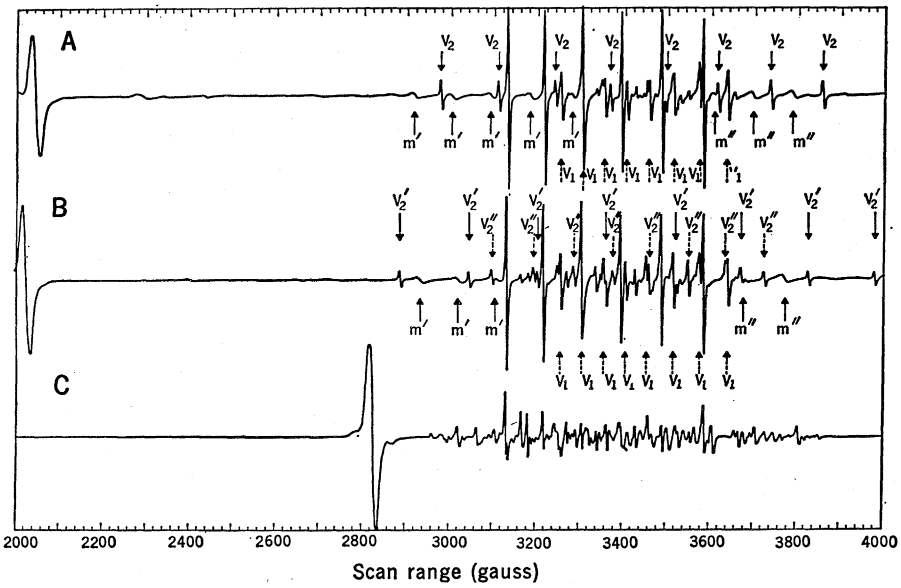

Fig. 2. Electron paramagnetic resonance spectra of the blue gem-quality zoisite crystal from Tanzania at 9.40 Ghz. (A) **H** parallel to **a**; (B) **H** in the (001) plane, 18° from the *a*-axis; and (C) **H** in the (010) plane, 30° away from the *a*-axis.

For **H** in the (100) and (001) planes at various angles, sharp six-line patterns due to the central ($-1/2 \rightarrow 1/2$) transition of Mn^{2+} were observed. However, for **H** in the (010) plane away from either the *a*- or the *c*-axis the six-line pattern splits up and broadens out, an indication that the point-group symmetry of Mn^{2+} is *m*, the (010) plane being the mirror plane.

Two types of V^{2+} central ($-1/2 \rightarrow 1/2$) transitions giving rise to eight-line patterns, denoted as V_1 and V_2 (Fig. 2), were also observed. Hyperfine splittings of both types of V^{2+} resonances are highly anisotropic. The angular variation of the V_1 hyperfine splitting indicates a site symmetry *m*, with (010) as the mirror plane. The system of principal axes of the V_1 spin Hamiltonian is identical with that of Mn^{2+}. Thus V^{2+} ions of type 1 probably occupy the same site as Mn^{2+}. The V_2 resonance lines are often obscured, and hence only a partial analysis can be made. Angular variation of the spectra indicated that the (010) plane is not a mirror plane at the V_2 site.

The single intense resonance line (Fig. 2) has been identified as the central transition in Fe^{3+}, since the chemical analysis of this crystal showed a considerable amount of Fe^{3+} [0.03 percent (by weight)]. Unfortunately, the satellites are too broad to be observable. The position of the central line of Fe^{3+} is strongly anisotropic. The angular variation of the line position indicates that the Fe^{3+} ions must occupy a site with symmetry *m*, (010) being the mirror plane.

In the zoisite structure there are two nonequivalent seven-coordinated Ca-sites, Ca(1) and Ca(2), both with site symmetry *m*, (010) being the mirror plane (*7*). The Ca(2)–O_7 polyhedron is considerably distorted, the average Ca(2)–O distance being 2.55 Å. Since Mn^{2+} is a $^6S_{5/2}$ type ion, it has no crystal-field stabilization in a distorted site. Furthermore, the average octahedral Mn^{2+}–O distance, 2.20 Å, indicates that the Ca(2)–O_7 polyhedron is too large for the Mn^{2+} ion. Hence all the Mn^{2+} ions are most likely located on the Ca(1)-site.

Since the V^{2+} ions of type 1 follow the Mn^{2+} ions closely in angular variations, they are probably also located on the Ca(1)-sites. The higher intensities of the V_1 set of lines indicate that V^{2+} ions prefer the Ca(1)-site. The V^{2+} ions of type 2 deviate from the mirror plane. Since the average Ca(2)–O distance, 2.55 Å, is large and the polyhedron is quite irregular (*7*), the type 2 V^{2+} ions probably occupy an interstitial site within the Ca(2)–O_7 polyhedron.

Because of the ionic charge and radius, the Fe^{3+} ions must be located on one of the two Al-sites, Al(I) and Al(II), with site symmetries 1 and *m*, respectively. Since the angular variation of the Fe^{3+} resonance lines shows the mirror plane symmetry, the Fe^{3+} ions probably occupy the Al(II)-site with site symmetry *m*. This is consistent with the larger and more distorted octahedral coordination at the Al(II)-site, the average Al(II)–O distance being 1.97 Å. The suggested ordering of the Fe^{3+} ions in the Al(II)-site in zoisite is also consistent with the strong site preference of Fe^{3+} ions in the comparable Al(III)-site in epidote, $Ca_2Al_2(Al,Fe)Si_3O_{12}(OH)$, which is monoclinic but structurally closely related to zoisite (*8*). However, the crystal field parameter, $|D|$, for the Fe^{3+} ion is 0.14 cm^{-1}, which is rather small as compared to the quadrupole coupling constant of 18.5 Mhz measured by nuclear magnetic resonance for ^{27}Al at the Al(II)-site (*9*), the largest value for ^{27}Al measured thus far. Furthermore, the principal axes of the magnetic tensor for Fe^{3+} do not coincide with those of the ^{27}Al electric field gradient tensors. This lack of coincidence probably means that the Fe^{3+} ions deviate from the Al-position within the octahedron, but still are located on the mirror plane (010). Since no other Fe^{3+} resonance lines have been observed, we conclude that the Al(I)-site is completely free of Fe^{3+} ions. However, this situation may change with considerably higher concentrations of Fe^{3+}.

SUBRATA GHOSE
TUNG TSANG*

Planetology Branch, National
Aeronautics and Space Administration,
Goddard Space Flight Center,
Greenbelt, Maryland 20771

References and Notes

1. A. Abragam and B. Bleaney, *Electron Paramagnetic Resonance of Transition Ions* (Clarendon Press, Oxford, England, 1970).
2. S. Ghose, "Applications of Nuclear and Electronic Resonance Spectroscopy in Mineralogy" (AGI Short Course Lecture Notes, American Geological Institute, Washington, D.C., 1969), pp. G1–G15.
3. ——— and P. Schindler, *Mineral. Soc. Amer. Spec. Pap.* **2**, 51 (1969).
4. P. Schindler and S. Ghose, *Trans. Amer. Geophys. Union* **50**, 357 (1969).
5. T. Wildeman, *Chem. Geol.* **5**, 167 (1970).
6. T. Ito, *X-Ray Studies on Polymorphism* (Maruzen, Tokyo, 1950), p. 59.
7. W. A. Dollase, *Amer. Mineral.* **53**, 1882 (1968).
8. T. Ito, N. Morimoto, R. Sadanaga, *Acta Crystallogr.* **7**, 53 (1954).
9. D. Brinkmann, J. L. Staehli, S. Ghose, *J. Chem. Phys.* **51**, 5128 (1969).
10. We thank Professor C. S. Hurlbut, Jr., Harvard University, for the loan of the gem-quality zoisite crystal from Tanzania; for a description of the crystal, see C S. Hurlbut, Jr., *Amer. Mineral.* **54**, 702 (1969). We also thank Dr. V. Manson, Museum of Natural History, New York, and J. S. White, Smithsonian Institution, Washington, D.C., for other zoisite crystals.

* Permanent address: Department of Physics, Howard University, Washington, D.C. 20001.

27 August 1970; revised 14 October 1970